Optimization of Tomato Slices Drying in a Continuous Infrared-Assisted Refractance Window™ Dryer Using Response Surface Methodology

Rezvani, Zeinab; Mortezapour*+, Hamid; Ameri, Mehran; Akhavan, Hamid-Reza
Department of Biosystems Engineering, Faculty of Agriculture, Shahid Bahonar University of Kerman, Kerman, I.R. IRAN

Selçuk Arslan
The University of Uludağ, Faculty of Agriculture, Department of Biosystems Engineering, Bursa, TURKEY

ABSTRACT: *The present work aimed to investigate the energy consumption and quality of tomato slices dried in an InfraRed-Assisted Reflectance Window[tm] (IRARW) dryer. The response surface methodology was used to optimize the experimental factors, including water temperature, infrared (IR) power, and belt speed based on specific energy consumption, IR fraction, contents of ascorbic acid, total phenolic, and total lycopene and color indices (L*, a*, b*, and H°). All factors, except the belt speed in the range of 0.278 - 0.37 mm/s, had significant effects on the performance parameters. The maximum measured value of specific energy consumption, IR fraction, contents of ascorbic acid, total phenolic, and total lycopene were 1.76 kWh/kg, 60.4%, 302.2 mg/100g, 708.07 mg GAE/100g, and 38.61 mg/100g, respectively. Rising the IR power led to an increase in a* and a decrease in L* values of the color indices. The optimum drying condition was determined to be at the temperature of 70 °C and the IR power of 500 W.*

KEYWORDS: *Tomato slices; Specific energy consumption; Infrared fraction; Quality indices.*

INTRODUCTION

Tomato is the second most produced vegetable in the world after potato, and it is a very perishable fruit. Drying is the most known technique for improving product shelf life and facilitating the storage of agricultural and food products [1]. The energy crisis, on the one hand, and growing demands for high-quality products, on the other hand, have increased the interest in developing novel methods of food drying. Spray and freeze dryers are recommended for high-quality product drying; however, the former operates at relatively high temperatures and is time-consuming. These drawbacks cause unwanted structural changes in the product [2].

InfraRed (IR) dryers which are preferred to the other common systems have such advantages as drying time reduction, product quality maintenance, and energy efficiency enhancement [3]. Regardless of the surface irregularities, the IR dryers can provide uniform heating and achieve high-quality products. Since the IR lamps

* *To whom correspondence should be addressed.*
+E-mail address: h.mortezapour@uk.ac.ir
1021-9986/2022/12/4181-4192 *12/$/6.02*

were easily attached to the other dryers, various combined IR drying systems were developed in the past decade.

Water-bed drying is relatively a new technology in which hot water provides the required thermal energy for drying the product via radiation, conduction, and convection. This type of dryer, known as refractance window™ dryer, was found to conserve energy consumption and reduce production costs compared to the spray and freeze dryers [3]. This technology can maintain the color, vitamins, and antioxidants of the final product due to the short time and low-temperature drying. By comparing the performance of a RW™ dryer for fruits and vegetable drying with that of the freeze-drying method, it was revealed that the quality and nutrients of the product are preserved at a high level with the RW™ dryer [3]. Physical properties of the yogurt powder produced by RW™ dryer, except the color indices, were better than that by freeze-drying. RW™ drying was also recommended as an effective way for fast and quality drying of fish silage [2].

In RW™ dryers, once the product surface gets dried, it behaves like a closed window, and does not allow the IR radiation to penetrate the product. This, along with the low conduction heat transfer coefficient of the material, reduces the drying rate significantly and limits the dryer capacity [4, 5]. This also caused a non-uniformity in the product moisture content, especially when they are thick. A significant drawback of the RW™ dryers, however, is the low operating capacity due to the thin film drying [6].

New drying technologies are innovative components of the conventional techniques that have emerged to meet the changing consumer and market needs [4]. To address the capacity problem of the RW™ dryers, the present study proposed an IR-Assisted RW (IRARW) dryer. The dryer was designed in such configuration to gain fast, energy-efficient, and quality drying benefits of the RW™ and IR dryers. Therefore, the main objective of the study is to develop and evaluate the continuous infrared-assisted RW™ dryer. In this respect, the present work aimed to optimize the designed IRARW dryer based on the parameters of energy consumption and quality of dried tomatoes. Therefore, the effects of the experimental parameters, including water temperatures, power of IR radiation, and conveyor belt speeds on specific energy consumption, IR fraction, the contents of ascorbic acid, total phenolic, and total lycopene and color indices (L^*, a^*, b^*, and $H°$) were investigated and optimized using the surface response methodology.

THEORETICAL SECTION

Description of the IRARW dryer

In order to investigate the combined influence of the IR power and RW™ drying on the tomato slices, a prototype continuous IRARW dryer was designed and developed at Biosystems Engineering Department of Shahid Bahonar University of Kerman, Iran. The system includes a hot water bed, stainless steel duct, transparent polyester (Mylar) conveyor belt, electromotor belt driver, hot water pump, blower, IR lamps, and auxiliary tank equipped with an electrical water heater. Figure 1 shows a schematic of the dryer.

The products are placed on the surface of the Mylar belt, which was tightly wrapped on the top of the hot water-bed in contact with the water surface. The selection of the Mylar film thickness was accomplished using the previous reports [7]. The electromotor moves the immersed Mylar film on the hot water. IR waves infiltrate into the product, resulting in a temperature difference between the inside and the surface, which in term, leads to an increase in the moisture flux and rapid saturation of the air surrounding the product surface. This results in moisture condensation inside the product and burns on the surface. For this reason, the IR dryers are usually supported with an airflow to move out the saturated air surrounding the product. To this end, a blower was installed on the duct to provide the required airflow throughout the process. Through the drying path, the product loses moisture and dries under the influence of the bottom hot water bed, the above IR lamps, and the airflow. The pump is employed to circulate the water between the hot water-bed and the tank, where the electric heater was installed. Technical properties of the dryer components are given in Table 1A and a photograph of the IRARW dryer is shown in Fig. 1.

Experimental procedure

Evaluation of the developed dryer was conducted at different water temperatures, IR powers, and belt speeds. In each test, fresh tomato slices (with the initial moisture content of 94.2 ± 0.6% wet basis) were placed on the belt to be dried.

The dryer performance was investigated based on the parameters of IR Fraction (IRF), specific energy consumption, color indices, Ascorbic Acid Content (AAC), Total Phenolic Content (TPC), And Total Lycopene Content (TLC) of the final product. The dried samples after each test were placed in polyethylene bags.

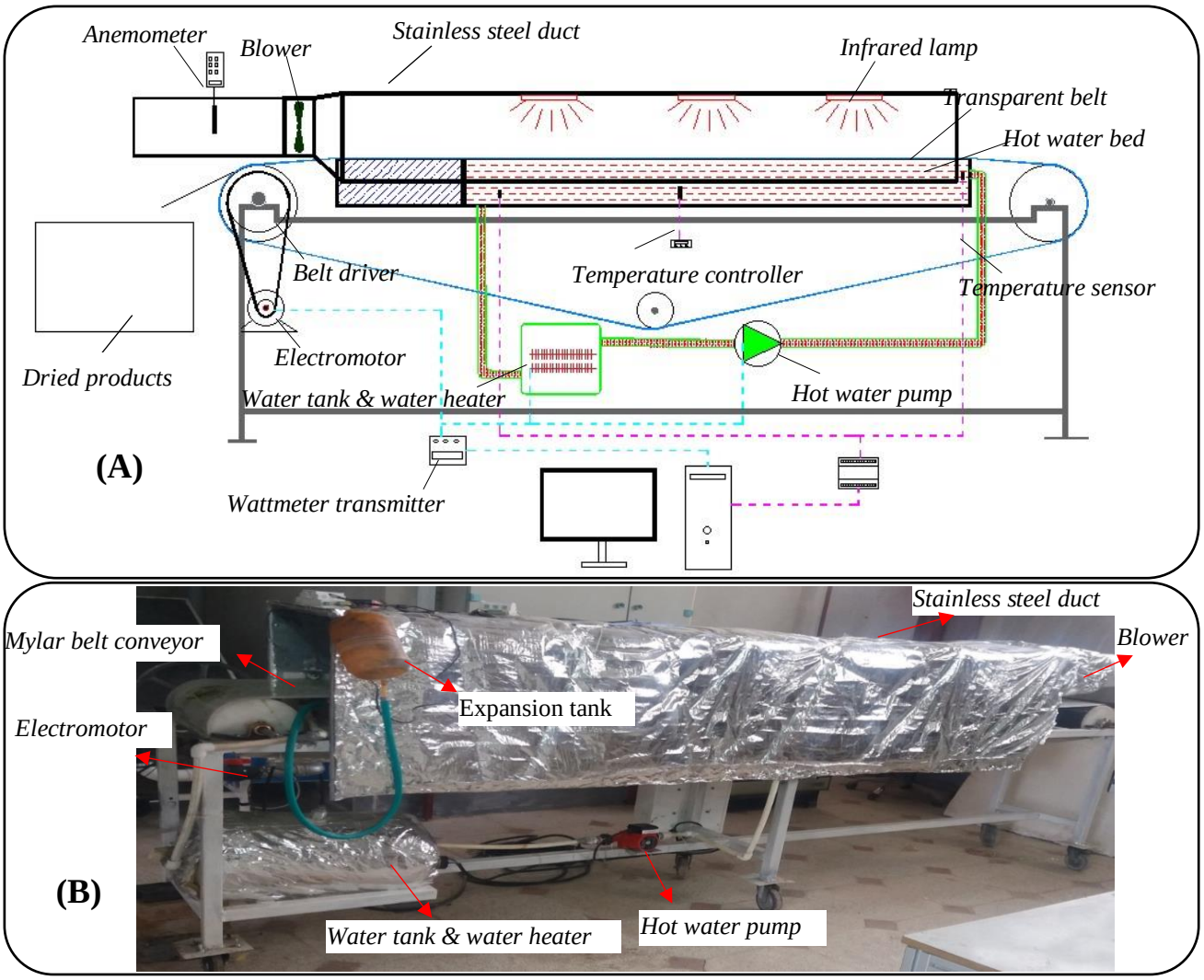

Fig. 1. A: A schematic of the continuous IRARW dryer B: A photograph of the IRARW dryer

The purpose of the experimental setup was to determine the conditions that will give the minimum SEC and the maximum IRF, AAC, TPC, and TLC values. To investigate the relationship between the dependent and the independent variables, the experiments were arranged based on the Response Surface Methodology (RSM). Central Composite Design (CCD), which was first described by [8] as the most popular experimental design method, was used for the RSM analysis. The independent variables, each of which came in five levels, were the water-bed temperature (60, 64, 70, 76, and 80 °C), belt speed (0.28, 0.29, 0.32, 0.35, and 0.37 mm/s), and IR lamp power (200, 280, 400, 520, and 600 W). The factors were chosen based on literature [9-14] and trials.

SEC, IRF, color indices, AAC, TPC, and TLC of the dried tomatoes were considered as the objective functions. The independent variables of water temperature, IR power, and belt speed are intended as A, B, and C, respectively, as well as their corresponding coded values ranging from -1 and +1. According to the CCD, the total number of experimental runs is determined as $20= 2^k+2k+6$, where k is the number of factors (k=3) and 6 is the number of replications at the design center to estimate the model error [15].

Throughout the optimization process, the responses are attributed to the independent variables by a quadratic model. The quadratic model can be written as [1, 16]:

$$\eta = \beta_0 + \sum_{j=1}^{k} \beta_j X_j + \sum_{j=1}^{k} \beta_{jj} X_j^2 + \sum_{i} \sum_{<j=2}^{k} \beta_{ij} X_i X_j + e_i \quad (1)$$

where η is the response, X_i and X_j are independent variables

(i=1 to k); β_o is a constant coefficient, β_j , β_{jj} , and β_{ij} (i and j=1 to k) are interaction coefficients of the linear, the quadratic, and the second-order terms, respectively; and e_i is the error. The experimental results have been evaluated by Design-Expert 7.0 to obtain the approximation functions of the dependent variables. The coefficients with the p-values higher than 0.05 were distinguished as non-significant, and therefore, omitted from the equation. Validation of the obtained models was carried out using the coefficient of determination (R^2) criterion.

Samples preparation

Fresh tomatoes were purchased from a local fruit and vegetable market in Kerman, Iran, in June 2019. Tomatoes with similar properties (color, size, shape, and texture) were selected, washed in chlorinated water (50 mg Cl_2/kg H_2O), drained, and stored in a refrigerator (temperature of 4 ± 1 °C). Approximately two hours before every experiment, 2 kg of tomatoes were placed in room temperature. Then, the tomatoes were sliced transversely at the thicknesses of 5±1 mm.

Parameters calculations

The dryer performance was investigated using IR fraction, specific energy consumption, and quality characteristics of tomato drying. The performance parameters' calculation was as follows:

Determination of energy consumption

The electrical energy needed for the auxiliary heater, the blower, the water pump, the electromotor, and the IR lamps counted for the total energy consumption of the system.

IRF shows the fraction of the total energy consumed by the IR lamps. The parameter was obtained using the following expression [17]:

$$IRF = \frac{E_{IR}}{E_T} \times 100 \quad (1)$$

Where, E_{IR} is the energy consumed by the IR lamps (kWh) and E_T is the total energy consumption (kWh).

SEC, which describes the amount of energy spent to remove one kg of water from the product, was calculated using Eq. (3) [18]:

$$SEC = \frac{E_T}{m_{wd}} \quad (2)$$

Where m_{wd} stands for the mass of the evaporated moisture during the drying process (kg).

Determination of quality characteristics

The color indices of the tomato slices, a^* for redness (green to red), L^* for lightness (white to black or light to dark), and b^* for yellowness (yellow to blue), were measured at each experiment using a colorimeter (TES 135A, TES Co., Taiwan). The hue angle was calculated as $H^o = \tan^{-1}(b^*/a^*)$ [19].

To determine AAC, 25 mL of a 10 g/L metaphosphoric acid solution was mixed with 2.50 g tomato powder, stirred for two hours, and then filtered through Whatman filter paper. Finally, 0.5 mL of the filtered sample was titrated using the 2,6-dichloroindophenol sodium salt [20]. The results were given as milligrams per 100 g of dry matter.

To determine the TPC, 5.0 g of dried slices were ground with a mortar and pestle and then 0.05 g of powder was mixed with 1 mL of methanol and vortexed for 30 min. The extract was filtered through Whatman filter paper. The TPC of the extract was measured by Folin-Ciocalteu as described by *Santos-Sánchez et al.* [20]. The results were represented as mg Gallic Acid Equivalents (GAE) per 100 g of dry matter.

To determine of TLC, 5.0 g of dried tomato was mixed with 1 mL distilled water and ground in a mortar. The TLC was determined by the method developed by Fish, Perkins-Veazie, and Collins as described by *Santos-Sánchez et al.* [20]. The results were presented as mg per 100 g of dm (dry matter).

Instrumentation

Water temperature, power consumption of the water heater, and flow rate of air were measured during the experiments. Two temperature sensors (SMT160) were located at the inlet and outlet of the hot water bed. A switched temperature controller (STC-100) was used to control the water temperature. A hot-wire anemometer (TES 1340, TES co., Taiwan) was used to measure the airflow rate. The energy consumption throughout the tests was determined using a wattmeter transmitter (TM-1510, Tika Co, Iran).

The standard uncertainty for the measurement instrument has been calculated using Eq. (4) [21]:

$$u = \frac{a}{\sqrt{3}} \quad (3)$$

Where a is the accuracy of the instrument. Technical specifications of the measurement instruments and the estimated uncertainties of the instrument are given in Table 1B.

Table 1: Technical specifications of the IRARW dryer (A) the measurement instrument and results of uncertainty analysis (B)

A	Dryer component	Detail		
Hot water bed		Dimensions: 0.4 m×1.95 m ×0.14 m		
Transparent polyester		Material: Mylar; Dimensions: 7 m× 0.4 m ×0.025 m		
Stainless steel duct		Dimensions: 0.52 m×0.7 m×3 m		
Hot water pump		Nominal power: 46 W, Flow rate: 0.5 L/min		
Blower		Nominal power: 40 W, Air flow rate: 0.05 m^3/h		
Electromotor		Nominal power:14 W; Rotational speed: 1 RPM		
Water heater		Maximum power: 2000 W		
B	Instrument (model)	Measured parameter	Accuracy	Uncertainty
Wattmeter (TM1510)		Electrical power consumption	± 1 W	0.58 W
Temperature sensor (SMT160)		Water temperature	± 0.7 °C	0.4 °C
Switched temperature controller (STC-100)		Water temperature controller	± 1 °C	0.58 °C
Hot-wire anemometer (TES-1341)		Air flow rate	±3%	1.73%

Table 2: Experimental conditions of the CCD runs and the corresponding results

Run	A	B	C	SEC kWh/kg	IRF (%)	L^*	a^*	b^*	H°	AAC (mg/100g)	TPC (mg GAE/100g)	TLC (mg/100g)
1	3	3	3	1.06	41.88	32.20	37.13	18.23	26.15	261.90	565.41	31.05
2	3	3	5	0.91	37.74	31.10	35.32	17.12	25.86	220.50	532.51	27.40
3	2	4	2	0.99	45.19	33.40	40.12	19.14	25.50	234.90	598.94	29.80
4	3	3	3	1.06	41.89	32.30	37.12	18.24	26.17	249.50	427.20	32.43
5	5	3	3	1.29	18.90	30.71	34.81	17.29	26.41	226.50	651.60	34.20
6	4	2	4	1.74	13.05	32.50	33.93	17.25	26.95	266.40	531.87	25.32
7	2	4	4	0.95	60.40	31.80	38.28	17.98	25.16	212.50	602.31	26.53
8	3	3	1	1.06	41.98	33.21	38.46	19.10	26.41	279.10	557.32	27.91
9	3	3	3	0.91	37.74	32.30	37.45	18.20	25.92	251.20	570.03	33.90
10	3	1	3	1.76	13.04	34.20	35.78	18.61	27.48	301.50	422.75	25.50
11	4	4	4	1.32	28.58	28.80	35.52	18.00	26.87	202.45	701.52	35.21
12	3	3	3	0.98	39.81	32.29	37.63	18.26	25.89	251.30	512.20	33.30
13	3	5	3	0.99	39.88	30.40	38.47	17.91	24.97	209.80	708.07	36.53
14	4	4	2	1.32	28.58	30.45	37.36	17.99	25.71	217.40	701.52	38.61
15	4	2	2	1.20	24.33	33.45	35.77	18.41	27.24	298.30	531.87	26.98
16	1	3	3	0.92	46.21	33.87	39.44	19.23	25.99	280.40	479.21	28.10
17	3	3	3	0.92	37.74	32.29	37.58	18.27	25.93	249.00	565.41	33.12
18	3	3	3	0.92	37.75	32.28	37.69	18.29	25.89	230.30	565.41	32.76
19	2	2	4	1.09	38.50	33.34	36.69	18.40	26.64	293.50	429.30	27.56
20	2	2	2	1.18	38.00	34.21	38.52	19.56	26.92	302.20	420.20	31.10

RESULTS AND DISCUSSION

Twenty runs were performed to illustrate the effects of water temperature, belt speed, and IR power on SEC, IRF, and quality indices of the dried tomatoes. The obtained results and the experimental conditions are given in Table 2.

The findings of the accompanying RSM study are given in Table 3A. In all parameters, the largest to smallest ratio of the response, were lower than 10, and therefore, data transformation was not required. The belt speed did not have a significant effect on any parameters. Consequently, all the figures are shown at the constant belt speed of 0.32 mm/s.

Table 3: Design summary of RSM analysis (A) and optimization results of experimental conditions (B)

A	Response	Name	Units	Minimum	Maximum	Ratio	Model	R^2
	Y1	SEC	kWh/kg	0.91	1.76	1.93	RQuadratic[1]	0.72
	Y2	IRF	%	13.04	60.4	4.63	RLinear[2]	0.77
	Y3	L^*	Dimensionless	28.8	34.21	1.19	R2FI[3]	0.85
	Y4	a^*	Dimensionless	33.93	40.12	1.18	RQuadratic	0.88
	Y5	b^*	Dimensionless	17.12	19.56	1.14	R2FI	0.79
	Y6	H^o	Dimensionless	24.97	27.48	1.10	RLinear	0.76
	Y7	AAC	mg/100g	202.45	302.20	1.49	RLinear	0.92
	Y8	TPC	mg/100g	420.2	708.07	1.69	RLinear	0.86
	Y9	TLC	mg/100g	25.32	38.61	1.52	R2FI	0.80

[1]Reduced Quadratic [2]Reduced Linear [3]Reduced 2FI

B	Water temp. (°C)	IR (W)	SEC (kWh/kg)		IRF (%)		AAC mg/100g		TPC mg GAE/100g		TLC mg/100g	
			P	E	P	E	P	E	P	E	P	E
	70	500	0.99	1.01	42.98	44.32	240.55	243.01	616.50	622.01	32.50	34.30

P: Predicted, E: Experimental

Specific energy consumption

By omitting the non-significant coefficients, the equation of SEC in terms of coded variables could be presented in the following way:

$$\mathrm{SEC} = +1.03 + 0.15\,\mathrm{A} - 0.14\mathrm{B} + 0.15\mathrm{B}^2 \qquad (5)$$

The highest experimental SEC value (1.76 kWh/kg) occurred in run No.10 (water temperature of 70 °C, and IR power of 200 W). The lowest value of SEC (0.91 kWh/kg) was observed in run No.2 (water temperature of 70 °C, and IR power of 400 W). Investigation of a liquid desiccant-assisted solar juice concentration system for barberry juice indicated the maximum and minimum SEC of 1.13 kWh/kg and 0.92 kWh/kg, respectively [22]. SEC values for potato drying using a microwave dryer are estimated to be between 1.17 kWh/kg and 2.93 kWh/kg [23]. The minimum SEC of 2.09 kWh/kg was reported for onions drying in a solar dryer equipped with the heat recovery system [24].

The influence of water temperature and IR power, at the constant belt speed of 0.32 mm/s, on the SEC was shown in Fig. 2. Clearly, SEC increased linearly with rising the water temperature. This is mainly due to the increment of the heat losses from the circulating water as a result of the raising the temperature difference between the water and the ambient. Furthermore, Fig. 2 shows that the effect of the IR power on SEC is inverse and quadratic. Results of a study on biomass drying in an IR-assisted hot air dryer indicated an inverse relationship between the IR power and the SEC values [25]. It was shown that raising IR power caused an increase in the product temperature, which in turn increased the drying rate and caused a decrease in drying time [26].

Effect of drying condition on the infrared fraction

The proposed RSM model for IRF was found to be linear as shown in Eq. (6):

$$\mathrm{IRF} = +35.56 - 9.77\,\mathrm{A} + 6.88\,\mathrm{B} \qquad (6)$$

The highest IRF value was 60.40% in run No.7 (water temperature of 64 °C, and IR power of 520 W), while the lowest IRF value (~ 13.04%) was observed in run No.10 (water temperature of 70 °C, and IR power of 200 W). Variation of IRF with water temperature and IR power at the belt speed of 0.32 mm/s is shown in Fig. 2. This figure demonstrates that the effects of water temperature and IR power on IRF are descending and ascending, respectively. Raising the water temperature increases the amount of energy consumed by the heater and thus reduces the IR fraction. On the other hand, the IR fraction increases with raising IR power.

Ascorbic acid content

The RSM model of the coded variables being proposed for AAC is linear and has been given as follows:

$$\mathrm{AAC} = +251.94 - 10.93\,\mathrm{A} - 32.77\,\mathrm{B} - 21 \qquad (7)$$

The minimum (202.45 mg/100g) and maximum (302.20 mg/100g) amounts of experimental AAC were observed respectively in run No.11 (water temperature of 76 °C,

and IR power of 520 W) and in run No. 20 (water temperature of 64 °C, and IR power of 280 W) [20]. reported that the AAC of fresh tomatoes was 360.70 mg/100g, and the AAC of dried tomatoes was in the range of 215-262.60 mg/100g [20]. According to Fig. 2, AAC increased as a result of a decrease in water temperature as well as IR power.

Similarly, an increment in temperature during tomatoes drying decreased the AAC content of dried samples [14]. Ascorbic acid is commonly considered as a heat and oxygen-sensitive compound. Heating and oxidation can accelerate the loss of ascorbic acid during the drying of agricultural products. As a result, the ascorbic acid level decreased slowly, following the rise in temperature [27]. However, the IR drying was a cost-effective and reliable way to preserve ascorbic acid among the drying processes, including sun drying, freeze-drying, hot-air drying, and vacuum drying [28].

Effect of drying conditions on the phenolic content

The following RSM model of coded variables was proposed to describe variations of TPC values.

$$TPC=+523.84+51.84\ A+85.89\ B \quad (8)$$

This model is a response surface reduced linear model. The highest experimental TPC (708.07 mg GAE/100g) of the dried tomato slices was obtained in run No.13 (water temperature of 70 °C, and IR power of 600 W). Fig. 2 shows the TPC of the dried tomato slices in the IRARW dryer at various IR power and water temperature. The TPC of dried samples increased with raising IR power. Infrared radiation not only improves the extraction of phenolic compounds through higher intermolecular interactions, but also accelerates the inter-conversion of undetectable compounds to detectable phenolic compounds [16]. It may also be due to the release of bound phenols with tomato matrix owing to the rupture of cell walls resulting from IR treatment along with the high temperatures used in drying-which enhance the increase of TPC.

Lycopene content

The changes in lycopene content in dried tomatoes at different levels of water temperature and IR power are shown in Fig. 2. The following RSM model of coded variables explains the TLC in dried tomatoes.

$$TLC=+30.87+1.57\ A+2.76\ B+2.98\ AB \quad (9)$$

The TLC in dried tomatoes was in the range of 25.32 to 38.61 mg/100g. The highest loss of experimental TLC occurred in run No. 6 (water temperature of 76 °C and IR power of 281 W). The maximum experimental TLC (38.61 mg/100g) was observed in run No.14 (water temperature of 76 °C and IR power of 520 W). Fig. 2, showed the increasing trend of the TLC with raising water temperature. As shown in Fig. 2, the TLC of tomato increased at elevated levels of IR power, and this could be ascribed to an increase in lycopene extractability or accessibility [29]. In addition, thermal processes can break down cell walls and weaken the bonding forces between lycopene and tissue, and in turn, increase lycopene release from the food matrix [30].

Color evaluation

The attractive red color of tomato products has a significant impact on consumer acceptance. However, processing methods may affect the lycopene pigments and decrease the color quality of the product [19]. Using the RSM method, the proposed models of coded variables for the color indicators are as follows:

$$L^*=+32.26-0.94A-1.13\ B-0.54\ AB \quad (10)$$

$$a^*=+37.15-1.38\ A+0.80\ B-0.089\ A^2-0.089\ B^2 \quad (11)$$

$$b^*=+18.27-0.49\ A-0.12\ B+0.15\ AB \quad (12)$$

$$H^o=+26.20+0.24\ A-0.64\ B \quad (13)$$

The color index of L^* is related to the brightness of the products. The lowest value of experimental L^* was 28.80 in run No. 11 (water temperature of 76 °C, and IR power of 520 W) and its highest value was 34.21 in run No. 20 (water temperature of 64 °C, and IR power of 280 W).

According to Fig. 3, the L^* values decreased when water temperature and IR power increased. The phenomenon results from an increase in browning reactions during the drying [19, 22]. This decreasing trend can be attributed to both reasons of polymerization of pigments and non-enzymatic browning reactions or the Maillard reaction at higher temperatures of the material during the drying process [31].

The red color of tomatoes and the color indice of a^* depend on the presence of lycopene pigments [32]. The largest and smallest values of experimental a^* (40.12 and 33.93) were obtained in run No.3 (water temperature of 64 °C, and IR power of 520 W) and in run No.6

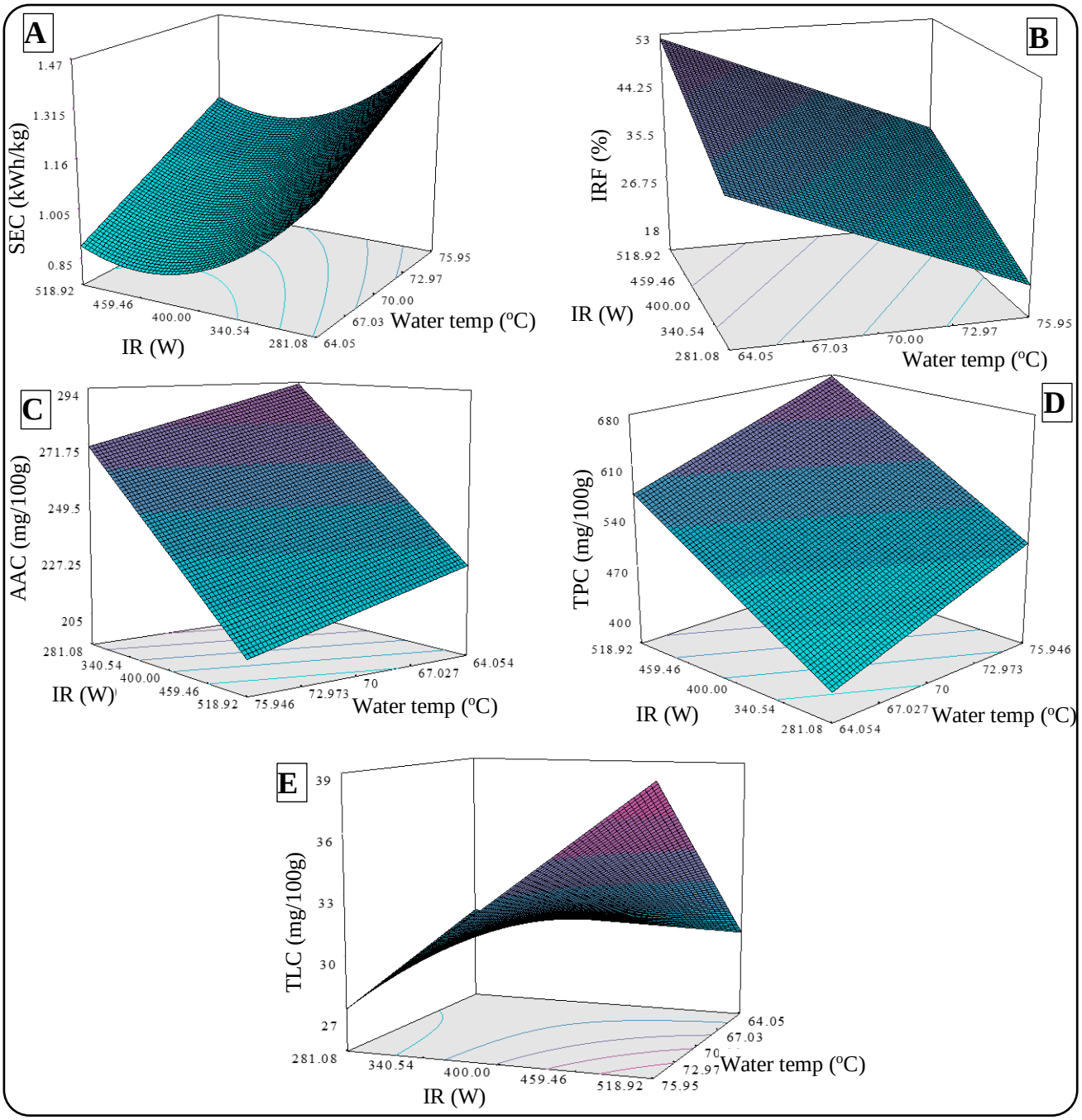

Fig. 2: Effect of water temperature and IR power on the energy consumption (SEC and IRF) and the quality characteristics (AAC, TPC, and TLC) of the tomato slices.

(water temperature of 76 °C, and IR power of 280 W), respectively. As shown in Fig. 3, the values of *a** decrease with increasing water temperature. In general; increasing the temperature has a destructive effect on the lycopene content and leads to a decrease in the *a** values. Oxidation and isomerization are the main reasons for the reduction of lycopene pigments during tomato processing [33]. In contrast, the increase in IR power led to an increase in the *a** values - a phenomenon which may be due to the improved lycopene extractability or accessibility [29]. Moreover, thermal processes can affect the lycopene-tissue bond by weakening their bonding forces, breaking down the cell walls in the food matrix, and releasing lycopene pigments from them [30].

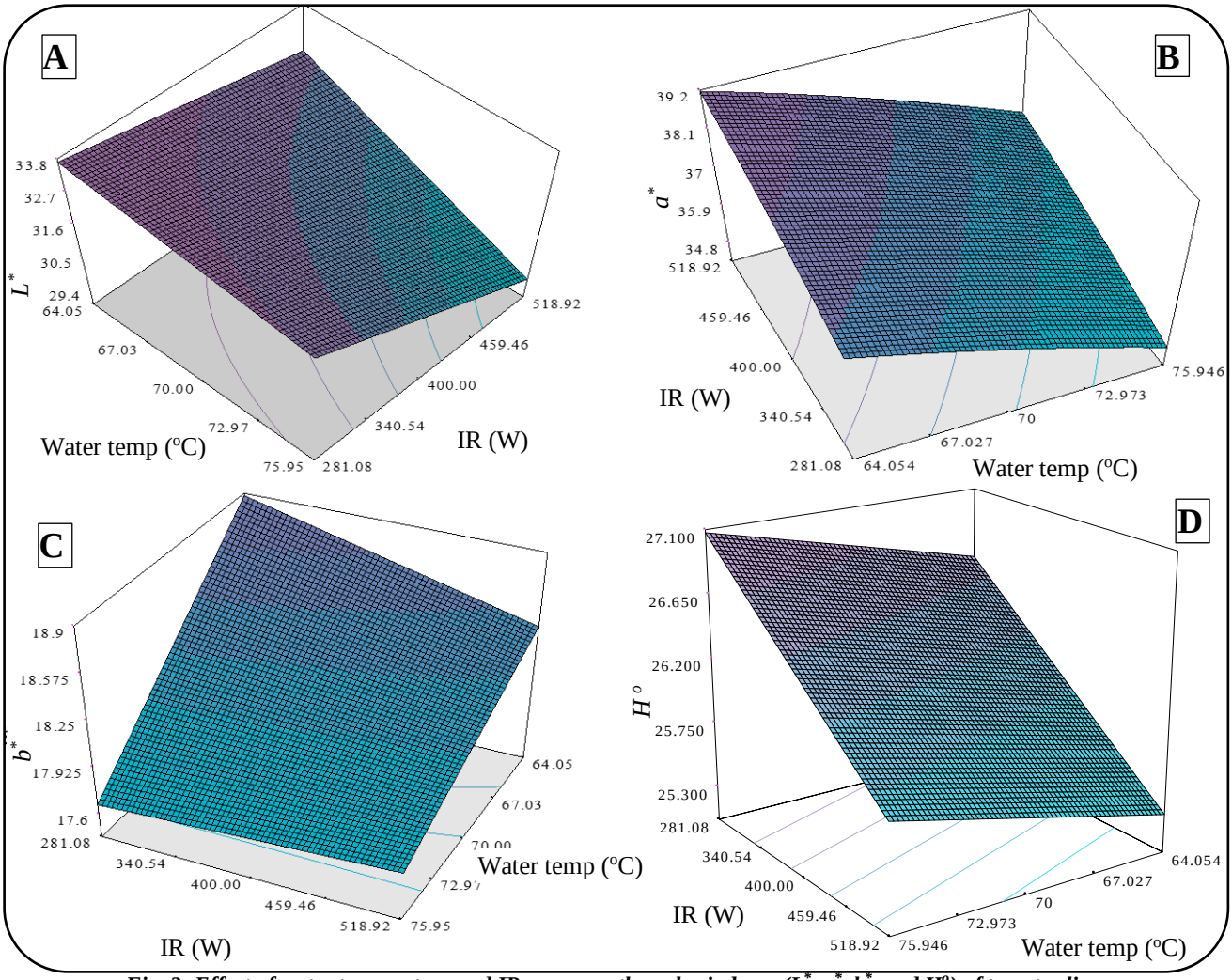

Fig. 3: Effect of water temperature and IR power on the color induces (L^*, a^*, b^*, and H^o) of tomato slices

The trend of changes in the b^* (Fig. 3), which is similar to the L^*, indicates that the yellowness of the tomato slices increases gradually.

The hue angle (H^o) represents the level of changes of the product surface color during the process. The H^o values of 0, 90, 180, and 270 stand for pure red, pure yellow, pure green, and pure blue, respectively [34]. The maximum and minimum experimental H^o values (27.48 and 24.97) were obtained in runs No.10 (water temperature of 70 °C, and IR power of 200 W) and No.13 (water temperature of 70 °C, and IR power of 600 W), respectively. The H^o values increased with rising water temperature and decreasing IR power (Fig. 3). Similar results were obtained in a previous study [34].

Optimization of experimental conditions

To determine the optimum operating condition of the designed dryer, AAC, TPC, and TLC values were supposed to be maximized and the SEC was kept minimized [35, 36]. The highest desirability was obtained at the water temperature of 70 °C and the IR power of 500 W. Table 3B shows the predicted and experimental values of the investigated parameters in the optimum condition of drying.

CONCLUSIONS

A continuous IR-assisted RW^{TM} (IRARW) dryer was investigated in the present study. The dryer performance was analyzed in terms of energy consumption and final product quality. To model the variations of the responses with the independent variables, and optimize the drying condition, the RSM technique was used. The following were concluded:

1. The SEC values increased linearly with raising the water temperature, whereas increasing the IR power caused a decrease in the SEC. The maximum values of IRF and SEC were 60.4% and 1.76 kWh/kg, respectively.

2. The effect of the IR power on IR fraction was quadratic and ascending.

3. The increase in water temperature decreased the a^* values. Raising the IR power increased the a^* values and lycopene content. Whereas the L^* values of tomatoes during the drying process declined with raising the water temperature and IR power.

4. AAC increased with decreasing the water temperature and the IR power. The highest AAC (302.20 mg/100g) during the experiments was measured at the water temperature of 64 °C, and IR power of 280 W.

5. The maximum experimental TPC of the dried tomatoes (708.07 mg GAE/100g) was measured at the water temperature of 70 °C, and IR power of 600 W. The TPC increased with raising the IR power as a linear function.

6. The maximum experimental TLC (38.61 mg/100g) was observed at the water temperature of 76 °C, and IR power of 520 W.

7. The optimum condition based on the lowest SEC and the highest IRF, AAC, TPC, and TLC values was achieved at the water temperature of 70 °C, and IR power of 500 W.

By comparing the findings of the present study with those of the previous ones, which investigated tomato slices drying, it can be concluded that the current developed system was able to accomplish the drying process satisfactorily. Furthermore, due to the relatively low energy consumption of the system, it can be beneficially equipped with solar (photovoltaic or thermal) collectors to work even independently of fossil fuels.

Acknowledgment

We acknowledge the financial support of Kerman Province Industrial Towns Company and Iran Small Industries and Industrial Towns Organization from this research project.

Nomenclature

Accuracy of the instrument	a
Redness (dimensionless)	a^*
Coded value of water temperature	A
Ascorbic acid content (mg/100g)	AAC
Coded value of IR power	B
Yellowness (dimensionless)	b^*
Coded value of belt speed	C
Dry matter	dm
Error	e_i
Energy consumed by the IR lamps (kWh)	E_{IR}
Total energy consumption (kJ)	E_T
Gallic acid equivalents	GAE
Hue angle (dimensionless)	$H°$
Infrared fraction (%)	IRF
Lightness (dimensionless)	L^*
Mass of the evaporated moisture during the drying process (kg)	m_{wd}
Specific energy consumption (kWh/kg)	SEC
Total phenolic content (mg GAE/100g)	TPC
Total lycopene content (mg/100g)	TLC
Standard uncertainty	u
Independent variables	X_i
Independent variables	X_j
Response	η
Constant coefficient	β_o
Interaction coefficients of the second-order term	β_{ij}
Interaction coefficients of the linear term	β_j
Interaction coefficients of the quadratic term	β_{jj}

Received: Oct. 3, 2021 ; Accepted: Jan. 31, 2022

References

[1] Ghasemi A., Chayjan R.A., Optimization of Pelleting and Infrared-Convection Drying Processes of Food and Agricultural Waste Using Response Surface Methodology (RSM), *Waste and Biomass Valorization*, **10(6):** 1711-1729 (2019).

[2] Van't Land M., Raes K., Refractance Window Drying of Fish Silage–an Initial Investigation into the Effects of Physicochemical Properties on Drying Efficiency and Nutritional Quality, *LWT*, **102:** 71-74 (2019).

[3] Bernaert N., Van Droogenbroeck B., Van Pamel E., De Ruyck H., Innovative Refractance Window Drying Technology to Keep Nutrient Value During Processing, *Trends in Food Science & Technology*, **84:** 22-24 (2018).

[4] Raghavi L., Moses J., Anandharamakrishnan C., Refractance Window Drying of Foods: A Review, *Journal of Food Engineering*, **222:** 267-275 (2018).

[5] Zotarelli M.F., Carciofi B.A.M., Laurindo J.B., Effect of Process Variables on the Drying Rate of Mango Pulp by Refractance Window, *Food Research International*, **69:** 410-417 (2015).

[6] Moses J., Norton T., Alagusundaram K., Tiwari B., Novel Drying Techniques for the Food Industry, *Food Engineering Reviews*, **6(3):** 43-55 (2014).

[7] Castoldi M., Zotarelli M., Durigon A., Carciofi B., Laurindo J., Production of Tomato Powder by Refractance Window Drying, *Drying Technology*, **33(12):** 1463-1473 (2015).

[8] Box G.E., Wilson K.B., On the Experimental Attainment of Optimum Conditions, *Journal of the Royal Statistical Society: Series B (Methodological)*, **13(1):** 1-38 (1951).

[9] Yusufe M., Mohammed A., Satheesh N., Effect of Duration and Drying Temperature on Characteristics of Dried Tomato (Lycopersicon Esculentum L.) Cochoro Variety, *Acta Universitatis Cinbinesis, Series E: Food Technology*, **21(1):** (2017).

[10] Obadina A., Ibrahim J., Adekoya I., Influence of Drying Temperature and Storage Period on the Quality of Cherry and Plum Tomato Powder, *Food science & nutrition*, **6(4):** 1146-1153 (2018).

[11] Correia A., Loro A., Zanatta S., Spoto M., Vieira T., Effect of Temperature, Time, and Material Thickness on the Dehydration Process of Tomato, *International Journal of Food Science*, **2015:** (2015).

[12] Kaur R., Kaur K., Ahluwalia P., Effect of Drying Temperatures and Storage on Chemical and Bioactive Attributes of Dried Tomato and Sweet Pepper, *LWT*, **117:** 108604 (2020).

[13] Corrêa P.C., de Oliveira G.H.H., Baptestini F.M., Diniz M.D.M.S., da Paixão A.A., Tomato Infrared Drying: Modeling and Some Coefficients of the Dehydration Process, *Chilean Journal of Agricultural Research*, **72(2):** 262 (2012).

[14] Demiray E., Tulek Y., Yilmaz Y., Degradation Kinetics of Lycopene, B-Carotene and Ascorbic Acid in Tomatoes During Hot Air Drying, *LWT - Food Science and Technology*, **50(1):** 172-176 (2013).

[15] Saeidi M., Ghaemi A., Tahvildari K., Derakhshi P., Exploiting Response Surface Methodology (RSM) as a Novel Approach for the Optimization of Carbon Dioxide Adsorption by Dry Sodium Hydroxide, *Journal of the Chinese Chemical Society*, **65(12):** 1465-1475 (2018).

[16] Jafari F., Movagharnejad K., Sadeghi E., Infrared Drying Effects on the Quality of Eggplant Slices and Process Optimization Using Response Surface Methodology, *Food Chemistry*, **333:** 127423 (2020).

[17] Mortezapour H., Ghobadian B., Minaei S., Khoshtaghaza M.H., Saffron Drying with a Heat Pump–Assisted Hybrid Photovoltaic–Thermal Solar Dryer, *Drying Technology*, **30(6):** 560-566 (2012).

[18] Coşkun S., Doymaz I., Tunçkal C., Erdoğan S., Investigation of Drying Kinetics of Tomato Slices Dried by Using a Closed Loop Heat Pump Dryer, *Heat and Mass Transfer*, **53(6):** 1863-1871 (2017).

[19] Dorouzi M., Mortezapour H., Akhavan H.-R., Moghaddam A.G., Tomato Slices Drying in a Liquid Desiccant-Assisted Solar Dryer Coupled with a Photovoltaic-Thermal Regeneration System, *Solar Energy*, **162:** 364-371 (2018).

[20] Santos-Sánchez N.F., Valadez-Blanco R., Gómez-Gómez M.S., Pérez-Herrera A., Salas-Coronado R., Effect of Rotating Tray Drying on Antioxidant Components, Color and Rehydration Ratio of Tomato Saladette Slices, *LWT-Food Science and Technology*, **46(1):** 298-304 (2012).

[21] Siddiqui F.R., Elminshawy N.A., Addas M.F., Design and Performance Improvement of a Solar Desalination System by Using Solar Air Heater: Experimental and Theoretical Approach, *Desalination*, **399:** 78-87 (2016).

[22] Alizadeh H.-R., Mortezapour H., Akhavan H.-R., Balvardi M., Performance of a Liquid Desiccant-Assisted Solar Juice Concentration System for Barberry Juice, *Solar Energy*, **184:** 1-10 (2019).

[23] Darvishi H., Energy Consumption and Mathematical Modeling of Microwave Drying of Potato Slices, *Agricultural Engineering International: CIGR Journal*, **14(1):** 94-102 (2012).

[24] Mortezapour H., Rashedi S., Akhavan H., Maghsoudi H., Experimental Analysis of a Solar Dryer Equipped with a Novel Heat Recovery System for Onion Drying, *J. Agr. Sci. Tech.*, **19:** 1227-1240 (2018).

[25] El-Mesery H.S., Abomohra A.E.-F., Kang C.-U., Cheon J.-K., Basak B., Jeon B.-H., Evaluation of Infrared Radiation Combined with Hot Air Convection for Energy-Efficient Drying of Biomass, *Energies*, **12(14):** 2818 (2019).

[26] Kocabiyik H., Tezer D., Drying of Carrot Slices Using Infrared Radiation, *International Journal of Food Science & Technology*, **44(5):** 953-959 (2009).

[27] Lemus-Mondaca R., Ah-Hen K., Vega-Gálvez A., Honores C., Moraga N.O., Stevia Rebaudiana Leaves: Effect of Drying Process Temperature on Bioactive Components, Antioxidant Capacity and Natural Sweeteners, *Plant Foods for Human Nutrition*, **71(1):** 49-56 (2016).

[28] Xu M., Tian G., Zhao C., Ahmad A., Zhang H., Bi J., Xiao H., Zheng J., Infrared Drying as a Quick Preparation Method for Dried Tangerine Peel, *International Journal of Analytical Chemistry*, **2017:** 1-11 (2017).

[29] Kocabiyik H., Yilmaz N., Tuncel N., Sumer S., Buyukcan M., Quality Properties, Mass Transfer Characteristics and Energy Consumption During Shortwave Infrared Radiation Drying of Tomato, *Quality Assurance and Safety of Crops & Foods*, **8(3):** 447-456 (2016).

[30] Dewanto V., Wu X., Adom K.K., Liu R.H., Thermal Processing Enhances the Nutritional Value of Tomatoes by Increasing Total Antioxidant Activity, *Journal of Agricultural and Food Chemistry*, **50(10):** 3010-3014 (2002).

[31] Serhat Turgut S., Küçüköner E., Karacabey E., Improvements in Drying Characteristics and Quality Parameters of Tomato by Carbonic Maceration Pretreatment, *Journal of Food Processing and Preservation*, **42(2):** e13282 (2018).

[32] Qiu J., Acharya P., Jacobs D.M., Boom R.M., Schutyser M.A., A Systematic Analysis on Tomato Powder Quality Prepared by Four Conductive Drying Technologies, *Innovative Food Science & Emerging Technologies*, **54:** 103-112 (2019).

[33] Shi J., Maguer M.L., Lycopene in Tomatoes: Chemical and Physical Properties Affected by Food Processing, *Critical Reviews in Food Science and Nutrition*, **40(1):** 1-42 (2000).

[34] Purkayastha M.D., Nath A., Deka B.C., Mahanta C.L., Thin Layer Drying of Tomato Slices, *Journal of Food Science And Technology*, **50(4):** 642-653 (2013).

[35] Zamani S., Rahimi M.R., Sadeghi H., Drying of Matricaria recutita Flowers in Vibrofluidized Bed Dryer: Optimization of Drying Conditions Using Response Surface Methodology, *Iranian Journal Chemistry and Chemical Engineering (IJCCE)*, **37(4):** 221-233 (2018).

[36] Taghinezhad E., Rasooli Sharabiani V., Kaveh M., Modeling and Optimization of Hybrid HIR Drying Variables for Processing of Parboiled Paddy Using Response Surface Methodology, *Iranian Journal Chemistry and Chemical Engineering (IJCCE)*, **38(4):** 251-260 (2019).